Repeatable and adjustable on-demand sciatic nerve block with phototriggerable liposomes

Alina Y. Rwei[a,b], Jung-Jae Lee[a,c], Changyou Zhan[a,c], Qian Liu[a,c], Meryem T. Ok[a,d], Sahadev A. Shankarappa[e], Robert Langer[c,f,1], and Daniel S. Kohane[a,c,1]

[a]Laboratory for Biomaterials and Drug Delivery, Department of Anesthesiology, Boston Children's Hospital, Harvard Medical School, Boston, MA 02115; [b]Department of Materials Science and Engineering, Massachusetts Institute of Technology, Cambridge, MA 02139; [c]David H. Koch Institute for Integrative Cancer Research, Massachusetts Institute of Technology, Cambridge, MA 02139; [d]Department of Biological Engineering, Massachusetts Institute of Technology, Cambridge, MA 02139; [e]Amrita Centre for Nanosciences and Molecular Medicine, Amrita Vishwa Vidyapeetham, Kochi, Kerala, 682041, India; and [f]Department of Chemical Engineering, Massachusetts Institute of Technology, Cambridge, MA 02139

Contributed by Robert Langer, September 24, 2015 (sent for review July 20, 2015)

Pain management would be greatly enhanced by a formulation that would provide local anesthesia at the time desired by patients and with the desired intensity and duration. To this end, we have developed near-infrared (NIR) light-triggered liposomes to provide on-demand adjustable local anesthesia. The liposomes contained tetrodotoxin (TTX), which has ultrapotent local anesthetic properties. They were made photo-labile by encapsulation of a NIR-triggerable photosensitizer; irradiation at 730 nm led to peroxidation of liposomal lipids, allowing drug release. In vitro, 5.6% of TTX was released upon NIR irradiation, which could be repeated a second time. The formulations were not cytotoxic in cell culture. In vivo, injection of liposomes containing TTX and the photosensitizer caused an initial nerve block lasting 13.5 ± 3.1 h. Additional periods of nerve block could be induced by irradiation at 730 nm. The timing, intensity, and duration of nerve blockade could be controlled by adjusting the timing, irradiance, and duration of irradiation. Tissue reaction to this formulation and the associated irradiation was benign.

pain | site 1 sodium-channel blocker | photosensitizer | light | near infrared

Current methods of treating pain, particularly orally taken opioid analgesics, can be limited in their effectiveness (1–3) and often induce side effects (3, 4). Recently, controlled release systems for local anesthetics have been developed to prolong nerve block and decrease systemic toxicity (5). These systems release drug in a continuous matter, so that the nerve block is prolonged until the payload is exhausted. However, the drug-release profile from such systems cannot be changed, irrespective of the patient's changing needs. Constant nerve block can be particularly troublesome at times when patient movement is required, because motor nerve block often accompanies the desired sensory nerve block (6, 7). A drug-delivery system that would allow on-demand nerve blockade therefore would be highly desirable.

Externally triggerable drug-delivery systems have been developed to provide such control over drug release. These systems can allow drugs to be released at the desired dosage, time, and location, enhancing the therapeutic effect and reducing side effects (8). A wide range of energy sources have been used as external triggers, such as light (9, 10), ultrasound (11), and magnetic fields (12). Light has been especially attractive because of the ease with which it can be controlled (with respect to wavelength, power, and duration of irradiation) and because it has been used in clinical medicine (13). A large number of light-triggerable drug-delivery systems has been reported (14–16), but relatively few have advanced as far as in vivo studies, in part because of limitations such as the poor tissue penetration of UV and visible light (16, 17).

Light-triggering drug release from carriers can be induced by photosensitizers that produce reactive oxygen species (ROS) (e.g., singlet oxygen [$^1O_2$]) upon irradiation (18, 19). The ROS subsequently react with the carrier to induce the release of encapsulated drugs (20). In particular, irradiation of photosensitizers within liposomes can produce singlet oxygen, which will cause peroxidation of unsaturated lipids (21). The formation of a new α-bond and a 1,5 hydrogen shift (22) will render the lipid hydrophilic, destabilizing the hydrophobic interactions that maintain liposome integrity (23, 24) and allowing the release of encapsulated drugs. For example, irradiation with visible light of photosensitizer-loaded liposomes containing unsaturated egg phosphocholine (EggPC) lipids induced the release of an encapsulated dye (25, 26). However, this specific approach could not be used for our purposes because visible light does not penetrate tissue well (27, 28). Near-infrared (NIR) light is much less absorbed by tissue chromophores (17, 27–30) than are UV and visible light; therefore, it penetrates deeper into tissue, reaching up to 10 cm through breast tissue or 4 cm through muscle tissue (30). To enable NIR-triggering of drug release from liposomes, we have encapsulated the NIR-absorbing photosensitizer 1,4,8,11,15,18,22,25-octabutoxyphthalocyaninato-palladium(II), $PdPC(OBu)_8$ (18), hereafter abbreviated "PS." We also modified the lipid composition to enhance triggerability. The ROS-sensitive lipid in the EggPC-based liposomes contained singly allylic hydrogens (31) [from methylene groups adjacent to one double bond, which can react with singlet oxygen to form lipid peroxides (32, 33)]. A higher reactivity with singlet oxygen can be achieved using lipids with biallylic hydrogens (from methylene groups adjacent to two double bonds) (34). Therefore, to increase the efficiency of the phototriggered reaction, a lipid that contained biallylic hydrogens, 1,2-dilinoleoyl-sn-glycero-3-phosphocholine (DLPC), was used in this study.

Here we have demonstrated proof of principle of a system that could safely provide on-demand externally triggered local anesthesia (Scheme 1). To do so, we loaded PS-containing

Significance

We demonstrate an injectable drug-delivery system that would allow patients to adjust the timing, duration, and intensity of local anesthesia in painful parts of the body. Such on-demand analgesia could greatly enhance the management of a variety of pain states. Light-sensitive liposomes containing the potent local anesthetic tetrodotoxin induced sensory and motor nerve block in vivo upon irradiation with a 730-nm laser. The timing, duration, and intensity of the nerve blockade were adjustable by the timing, irradiance, and duration of irradiation. Tissue reaction to the formulation and associated irradiation was benign.

Author contributions: A.Y.R., J.-J.L., C.Z., R.L., and D.S.K. designed research; A.Y.R., J.-J.L., C.Z., Q.L., and M.T.O. performed research; A.Y.R., J.-J.L., and Q.L. contributed new reagents/analytic tools; A.Y.R., J.-J.L., C.Z., Q.L., M.T.O., S.A.S., R.L., and D.S.K. analyzed data; and A.Y.R., J.-J.L., C.Z., Q.L., M.T.O., S.A.S., R.L., and D.S.K. wrote the paper.

The authors declare no conflict of interest.

[1]To whom correspondence may be addressed. Email: rlanger@mit.edu or daniel.kohane@childrens.harvard.edu.

This article contains supporting information online at www.pnas.org/lookup/suppl/doi:10.1073/pnas.1518791112/-/DCSupplemental.

liposomes with the site 1 sodium-channel blocker tetrodotoxin (TTX), which is a potent local anesthetic with minimal myotoxicity (35) and neurotoxicity (36). TTX is very hydrophilic and therefore readily encapsulated within liposomes, like some other site 1 sodium-channel blockers (6, 7). Liposomes were selected as the drug-delivery vehicle because of their biocompatibility, injectability, acceptable drug-loading levels, and track record of clinical use and safety (37, 38). To enhance the encapsulation of TTX, which contains a positively charged guanidinium group (39), a negatively charged lipid, 1,2-distearoyl-sn-glycero-3-phosphatidylglycerol (DSPG), was added in the liposome formulation, as we have done in encapsulating other cationic site 1 sodium-channel blockers (6, 7). Saturated lipids were added to the liposome formulation (at a 1:1 molar ratio to the unsaturated lipids) to decrease the fluidity of the liposome bilayer and enhance liposome stability in physiological conditions (40, 41).

Results

Phototriggered Lipid Peroxidation. PS was synthesized (18) and showed the expected absorption peak at 729 nm in ethanol (*SI Appendix*, Fig. S1) (18). To assess the photostability of the PS, its ethanolic solution was irradiated for 15 min at 730 nm, 50 mW/cm^2. The spectrophotometric spectrum showed that 98% of the absorbance at 729 nm was preserved (*SI Appendix*, Fig. S1), suggesting that PS would have high photostability within the durations of irradiation intended in this work.

To demonstrate the feasibility of the proposed phototriggering mechanism, a mixture of DLPC and PS was irradiated in ethanol at 730 nm (50 mW/cm^2). A new absorption peak at 233 nm (*SI Appendix*, Fig. S2*A*) suggested the formation of conjugated dienes, products of lipid peroxidation (42, 43). The peak at 233 nm gradually increased with irradiation time. Irradiation of DLPC alone in ethanol did not show an increase in absorbance at 233 nm (*SI Appendix*, Fig. S2*B*), nor did the absorbance increase when irradiating PS alone in ethanol (*SI Appendix*, Fig. S2*C*), showing that the presence of both DLPC and PS was necessary for the phototriggered reaction.

PS was encapsulated in liposomes (Lipo-PS) (*SI Appendix*, Table S1) consisting of unsaturated lipid (DLPC), saturated lipid (1,2-distearoyl-sn-glycero-3-phosphocholine; DSPC), 1,2-distearoyl-sn-glycero-3-phosphatidylglycerol (DSPG), and cholesterol at a molar ratio of 3:3:2:3, with a mean diameter of 5.0 μm and a mean loading efficiency of 90%. The absorption spectrum of Lipo-PS showed a peak at 729 nm (Fig. 1*A*), whereas liposomes without PS (hereafter, "Lipo") showed negligible absorbance at 729 nm (*SI Appendix*, Fig. S3). Lipo-PS was green, and Lipo was white to visual inspection.

Singlet oxygen production from Lipo-PS was determined using 9,10-dimethylanthracene (DMA), a fluorescent probe that has been used to detect singlet oxygen production in liposomal membranes (44, 45). Fluorescent DMA undergoes cycloaddition specifically with singlet oxygen to form a nonfluorescent endoperoxide (46). DMA-loaded Lipo-PS showed the expected fluorescence peaks at 407 nm and 430 nm (*SI Appendix*, Fig. S4) (44). Upon 1-min irradiation (730 nm, 50 mW/cm^2), the fluorescence peaks attributed to DMA decreased by 85% (*SI Appendix*, Fig. S4*A*), whereas DMA-loaded Lipo showed a negligible difference in fluorescence upon irradiation (*SI Appendix*, Fig. S4*B*), suggesting that singlet oxygen was generated from PS in the liposomal environment.

Phototriggered lipid peroxidation in the liposomes was assessed by following the absorption spectra of Lipo-PS and Lipo. Upon irradiation of Lipo-PS (730 nm, 50 mW/cm^2) (Fig. 1*B*), a new absorption peak at 238 nm was observed, which increased with time, indicating progressive peroxidation with completion after ~5 min. The peak in the aqueous liposome solution at 238 nm corresponds to that at 233 nm in ethanolic solution (*SI Appendix*, Fig. S2*A*) and similarly indicates the formation of conjugated dienes (47), whereas the difference in peak absorption wavelength is caused by the different solvent (*SI Appendix*, Fig. S5*A*). Absorption peak shifts caused by the effect of solvents on the electronic excitations of organic molecules have been described (48). When Lipo was irradiated,

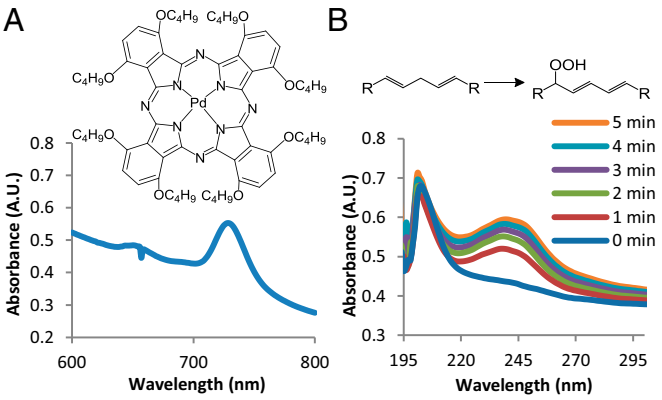

Fig. 1. Properties of the photosensitizer (PS) and phototriggered lipid peroxidation. (*A*) Structure of PS and absorption spectrum of Lipo-PS. (*B*) Chemical structures of the peroxidation reaction and absorption spectra of Lipo-PS with and without increasing durations of irradiation (730 nm, 50 mW/cm^2) in PBS. A.U., arbitrary units.

there were negligible changes at 238 nm (*SI Appendix*, Fig. S3). The kinetics of DLPC peroxidation was faster in the liposome system (time scale of minutes) than in organic solvent (time scale of hours), presumably because the local concentrations of PS and DLPC were higher in the phospholipid bilayer than in ethanolic solution. Ninety-seven percent of PS was preserved when Lipo-PS was irradiated (730 nm, 50 mW/cm^2) for 15 min, as determined by the minimal change in the absorbance at 729 nm (*SI Appendix*, Fig. S5*B*), indicating high photostability within the duration of treatment.

Drug Encapsulation and Phototriggered Release. Prior to experiments where local anesthetics were loaded into the liposomes, a hydrophilic fluorescent dye, sulforhodamine B, was used as a hydrophilic model compound to understand the release kinetics of the phototriggerable liposomes (*SI Appendix, Materials and Methods*). Sulforhodamine B-loaded liposomes (Lipo-PS-SRho) released the encapsulated dye upon irradiation repeatedly (*SI Appendix*, Fig. S6). These results also demonstrated that triggerable release from the liposomes is not restricted to TTX alone.

The site 1 sodium-channel blocker TTX was loaded into PS multivesicular liposomes (Lipo-PS-TTX) (*Methods* and Fig. 2*A*) with a mean size of 5.6 μm and a mean TTX-loading efficiency of 24% (*SI Appendix*, Table S1). There was no degradation of TTX (measured by ELISA) for irradiation times up to 15 min (*SI Appendix*, Fig. S8), indicating high TTX stability during the light-induced production of singlet oxygen.

Release of TTX from liposomes was studied by dialyzing 100 μL of Lipo-PS-TTX against 14 mL of PBS (Fig. 2*B*). In the absence of irradiation, there was an initial burst release of 5% of total TTX, followed by slower release. Irradiation (730 nm, 50 mW/cm^2, 10 min) at the 5-h time point triggered release 5.6% of TTX over the ensuing 2 h, followed by a return to a slower baseline. A second irradiation event at the 9-h time point released 5.4% of TTX over the next 2 h. These results showed that the release of TTX could be controlled by light. TTX-loaded liposomes that did not contain PS (Lipo-TTX) showed no difference in release kinetics when irradiated (Fig. 2*C*), demonstrating the importance of PS in the phototriggered release of TTX. These results demonstrated on-demand, repeated triggering of release of TTX from Lipo-PS-TTX in vitro.

Cytotoxicity. The cytotoxicity of formulations (*SI Appendix*, Fig. S9) was assessed in two cell lines relevant to local anesthetic-related tissue injury (6): C2C12 cells (a myotube cell line) and PC12 cells (a pheochromocytoma line frequently used for testing of neurotoxicity). Cells were incubated for 96 h in 900 μL of medium with 100 μL of test materials placed above them in Transwells.

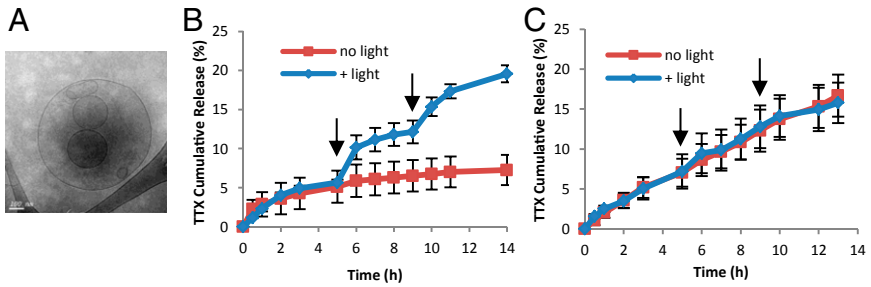

Fig. 2. TTX-loaded liposomes. (*A*) Cryo-transmission electron microscopy image of Lipo-PS-TTX. (*B*) Release of TTX from Lipo-PS-TTX at 37 °C with and without irradiation (730 nm, 50 mW/cm^2, 10 min) at the time points (5-h and 9-h) indicated by arrows. (*C*) Release of TTX from Lipo-TTX. Irradiation (730 nm, 50 mW/cm^2, 10 min) at the 5-h and 9-h time points did not increase TTX release. Data are means ± SD, $n = 4$.

All groups in both cell types maintained cell viability >90% compared with cells that were not exposed to particles. Viability was 17.4% and 11.8% lower in C2C12 and PC12 cells, respectively, when exposed to irradiated (730 nm, 50 mW/cm^2, 15 min) Lipo-PS-TTX particles than in cells exposed to irradiated Lipo-TTX particles ($P < 0.0125$) (*SI Appendix*, Fig. S9).

Sciatic Nerve Blockade. Liposomes were injected at the sciatic nerve, then the animals underwent neurobehavioral testing that examined sensory and motor function. In sensory testing, the thermal latency (explained in *Methods*) was measured at predetermined intervals. Latency is a measure of the intensity of sensory nerve blockade (49, 50); normal latency is 2 s, and 12 s is the maximum allowed latency; after 12 s the hind-paw is removed manually from the hot plate to prevent thermal injury. The duration of nerve blockade was calculated as the time for latency to return to 7 s, the midpoint between the baseline (2 s) and the maximum (12 s). Animals also underwent neurobehavioral testing after irradiation events.

Injection of Lipo-PS-TTX at the rat sciatic nerve induced nerve blockade lasting 13.5 ± 3.1 h (values are expressed as mean ± SD unless otherwise stated) (Fig. 3*A*). Twenty-four hours after injection the injection site was irradiated with a 730-nm laser at 330 mW/cm^2 for 15 min; this irradiation induced a return of nerve block that lasted 2.8 ± 0.9 h. Lipo-TTX induced an initial nerve block lasting 14.6 ± 6.8 h, but subsequent irradiation did not cause nerve block, demonstrating that PS is necessary for the increase in hind-paw thermal latency upon irradiation(s). Lipo-PS

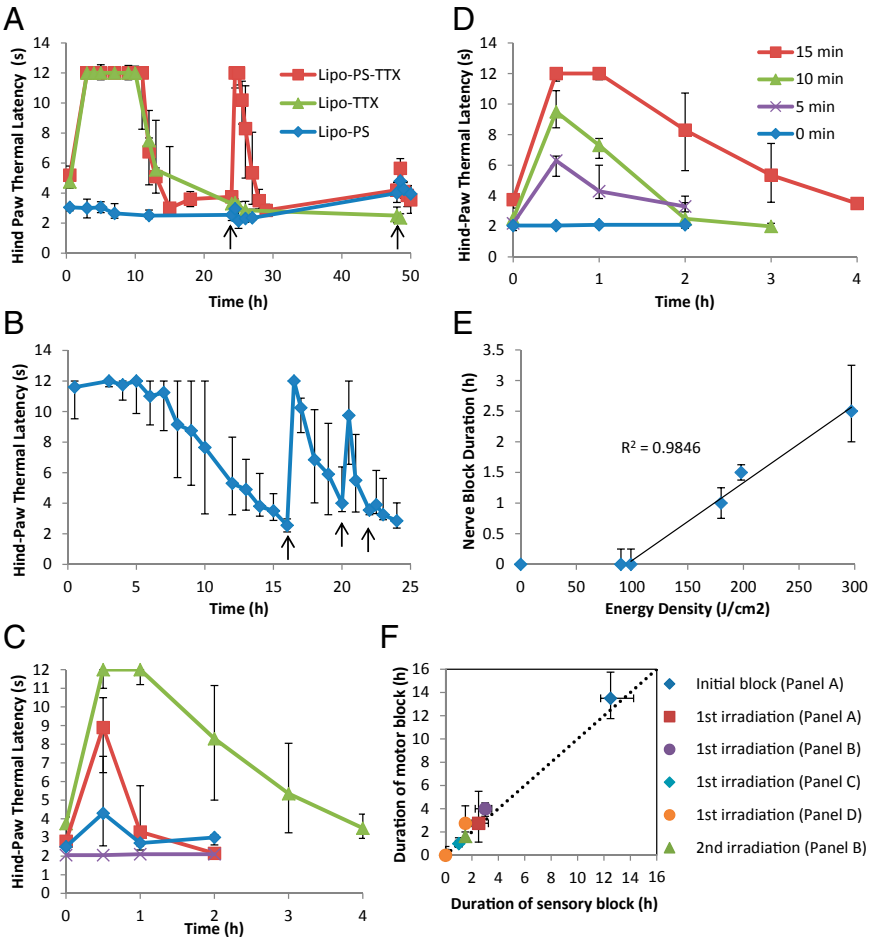

Fig. 3. Phototriggered nerve blockade in vivo. Animals were injected with liposomes at the sciatic nerve and then underwent neurobehavioral testing. The *y* axis (thermal latency) is a measure of nerve block; 2–4 s is baseline, and 12 s reflects deep nerve blockade. Irradiation events are indicated by black arrows. (*A*) External triggerability of different liposomal formulations upon irradiation (730 nm, 330 mW/cm^2, 15 min) at 24 h and 48 h. (*B*) Triggerability of Lipo-PS-TTX upon irradiation (730 nm, 330 mW/cm^2, 15 min) upon return of latency to baseline, at 16, 20, and 22 h. (*C*) Effect of irradiation on nerve blockade from Lipo-PS-TTX. Irradiation events were at 730 nm for 15 min and occurred 24 h after injection, after the initial block wore off. Green: 330 mW/cm^2; red: 200 mW/cm^2; blue: 100 mW/cm^2; purple: no irradiation. (*D*) Effect of the duration of irradiation on nerve blockade by Lipo-PS-TTX. Irradiation events were at 730 nm at 330 mW/cm^2 and occurred 24 h after injection, after the initial block wore off. (*E*) Effect of irradiance energy density on the duration of the nerve block induced by Lipo-PS-TTX using a 730-nm laser. Nerve block duration was defined as the duration of latency above 7 s. (*F*) Duration of sensory and motor nerve block in animals injected with Lipo-PS-TTX in *A*–*D*. The dotted diagonal line indicates identical durations of sensory and motor block. Data are medians ± quartiles, $n = 4$.

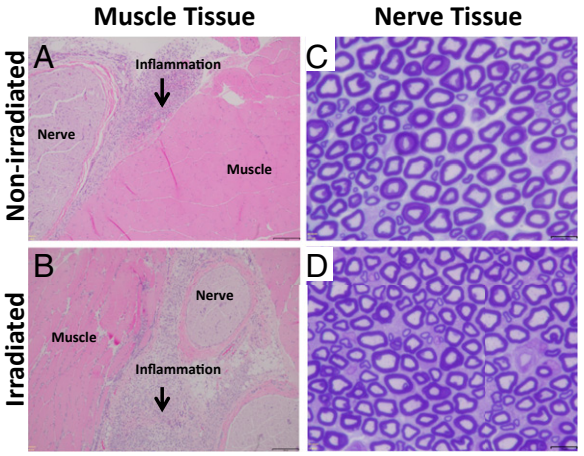

Fig. 4. Histology of rat tissue injected with Lipo-PS-TTX 4 d after the second irradiation event. (*A* and *B*) Representative light micrographs of H&E-stained tissue without (*A*) and with (*B*) irradiation (730 nm, 330 mW/cm^2, 15 min). (Scale bars, 100 μm.) (*C* and *D*) Representative photomicrographs of sections of sciatic nerve from animals without (*C*) and with (*D*) irradiation stained with toluidine blue. (Scale bars,10 μm.)

did not result in nerve block, with or without irradiation, indicating that the photosensitization reaction itself did not cause nerve block. Forty-eight hours after injection, a second irradiation at the injection site for 15 min induced a slight increase in latency only in animals injected with Lipo-PS-TTX. Animals treated with irradiation showed no sign of skin injury.

In subsequent experiments, we demonstrated that the timing, intensity, and duration of irradiation could be varied to adjust the intensity and duration of local anesthesia. Irradiation events (730 nm, 15 min, 330 mW/cm^2) could be clustered so that there was return of nerve blockade as soon as the previous nerve block wore off (Fig. 3*B*). The first irradiation event induced a nerve block lasting 3.3 ± 2.2 h; the second irradiation event produced a nerve block lasting 1.3 ± 1.0 h. The last irradiation event induced only a slight increase in latency. The cumulative duration of nerve blockade was ∼24 h. That the effect of the second irradiation event on nerve block depended on when it was performed (Fig. 3 *A* and *B*) suggests that there was ongoing basal release of TTX. These results and those in Fig. 3*A* show that this approach allows considerable control over the timing of nerve blockade.

It would be useful for patients to be able to tune the intensity and duration of nerve blockade. In these experiments, the irradiation events took place 24 h after injection, approximately 10 h after the initial nerve block had worn off. Irradiation for 15 min at 100 mW/cm^2 induced a slight increase in thermal latency (Fig. 3*C*), whereas increasing the power density to 200 mW/cm^2 or to 330 mW/cm^2 increased the thermal latency and the duration of block (to 2.8 ± 0.9 h). The magnitude and duration of block also could be controlled by varying the duration of irradiation (Fig. 3*D*). The duration of the nerve block had a linear relationship with energy density (the product of irradiance and irradiation duration) (Fig. 3*E*). Energy densities lower than 99 J/cm^2 did not result in nerve block as defined here (which requires a thermal latency above 7 s), but as the energy density increased above 99 J/cm^2 the nerve block duration increased linearly, indicating that nerve block duration can be controlled by the dosage of light.

Durations of motor nerve block and sensory nerve block were similar in all groups (Fig. 3*F*), whether induced by the initial injection or by subsequent irradiation and irrespective of the irradiance and duration of irradiation. This similarity is indicated by the proximity of all data points to the line of unity running diagonally across the plot.

Tissue Reaction. The sciatic nerves and surrounding tissues were harvested 4 d after the last irradiation event. All rats injected with PS-loaded particles had green particle deposits surrounding the sciatic nerve; rats injected with liposomes that did not contain PS had white particle deposits. These findings demonstrated that the liposomes were injected accurately at the target site.

Muscle tissue was processed with H&E staining, and nerve tissue was processed with toluidine blue staining (51, 52). Irradiated tissues (with no particles injected) did not show inflammation or myotoxicity (Table 1). In all cases where particles were injected, there was a mild localized inflammatory response with macrophages and neutrophils at the site of injection (Fig. 4 *A* and *B*). Foamy macrophages were observed, reflecting the uptake of injected liposomes. Deeper layers within the muscle had normal morphology without any signs of inflammation. Inflammation and myotoxicity scores were low in all groups. The only statistically significant difference between groups was between the inflammation scores in the light-only group (without liposome injection) and the irradiated Lipo-PS group. There were no statistically significant differences between groups in terms of myotoxicity (Table 1).

Nerve histology showed normal axonal distribution and myelin structure in all but one rat injected with Lipo-PS-TTX (Fig. 4 *C* and *D*). That rat, irradiated for 15 min at 330 mW/cm^2, exhibited perineural edema (*SI Appendix*, Fig. S10).

Discussion

We have demonstrated proof of principle of externally triggerable nerve blockade using an injectable drug-delivery vehicle that releases encapsulated local anesthetics upon NIR irradiation. Control of drug (TTX) release was achieved with distinct on- and off-states, and in vivo results showed that temporal control of sciatic nerve block could be achieved through externally controlled irradiation. Both Lipo-PS-TTX and Lipo-TTX induced block of more than 10 h upon administration, presumably from passive release of TTX (the initial burst release) after injection. After the initial nerve block wore off, irradiation of Lipo-PS-TTX induced nerve block, but irradiation of Lipo-TTX did not, suggesting that subsequent releases of TTX resulted from PS-mediated external triggering. Lipo-PS did not result in nerve block, whether irradiated or not, demonstrating that TTX is necessary for block and, in particular, that the irradiation of PS is not responsible for the nerve block.

The system described here has several appealing characteristics for treating pain in the perioperative period. First, the initial injection would provide an extended period of dense analgesia immediately after (or even during) the operative procedure. Subsequently, the patient would be able to trigger local anesthesia at will, to provide either relatively continuous anesthesia (Fig. 3*B*) or intermittent nerve block (Fig. 3*A*), as needed. Moreover the patient would be able to adjust the intensity and duration of nerve blockade by varying the intensity and duration (the energy density) of applied light. The linear relation between the duration of nerve block and energy densities higher than

Table 1. Tissue reaction

Liposome injection	Light/no light	Median inflammation score (range)	Median myotoxicity score (range)
Lipo-PS-TTX	No light	1 (0.75–1)	0 (0–0)
	+ light	2 (1.5–2)	0.5 (0–1)
Lipo-TTX	No light	1 (0.5–1.5)	0 (0–0.5)
	+ light	1 (0.75–1.25)	0 (0–0.25)
Lipo-PS	No light	1.5 (0.75–2)	0 (0–0)
	+ light	2 (2–2.5)*	0.5 (0–1.75)
No liposome	+ light	0 (0–0)*	0 (0–0)

Data are median with 25th and 75th percentiles (n = 4). Inflammation scores range: 0–4; myotoxicity scores range: 0–6. + light, irradiation performed with a 730-nm laser at 330 mW/cm^2 for 15 min. *P = 0.001 for comparison between the two groups. P values < 0.005 were considered statistically significant.

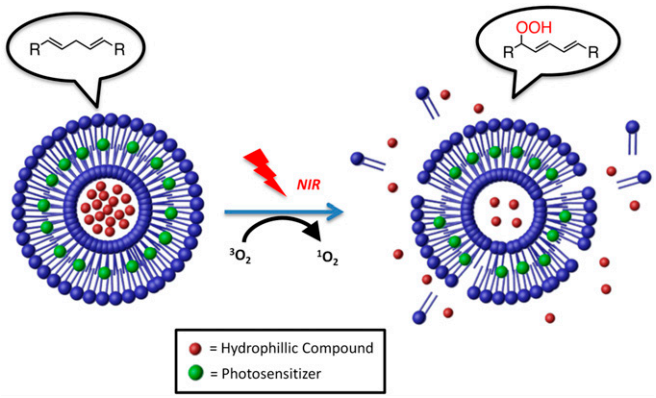

Scheme 1. Schematic of phototriggered cargo release from liposomes. PS and a hydrophilic compound (TTX) were encapsulated inside the liposomes. Upon NIR, singlet oxygen was produced and induced lipid peroxidation, which destabilized the liposome, leading to the release of TTX.

99 J/cm^2 suggests that control of the effects of irradiation might be straightforward. We were able to achieve well-defined degrees of anesthesia (latencies <12) by modulating the intensity and duration of anesthesia (Fig. 3 *C* and *D*), suggesting that it should be possible to induce specified submaximal degrees of anesthesia for extended periods by using low irradiances for long times or by using initially relatively high irradiances with a decrescendo pattern over time. The easy adjustability together with the ability to maintain particular degrees of anesthesia would be very useful in treating postoperative and other kinds of pain, where the degree of pain may vary with the level of activity, position, time of day, and other factors.

NIR light can penetrate tissues up to the centimeter scale (30) and therefore could reach many nerves in humans. However, the penetration depth of NIR light depends on the type of tissue within the light-penetration pathway (28) because of the difference in the absorption and scattering of light (i.e., attenuation) by various tissues. Consequently, the applicability of NIR light in targeting nerves in humans could be affected by the depth of the target nerve and the patient's physical condition (e.g., edema, obesity, hematoma, and scar tissue, among others) as well as the specific wavelength of light used.

The durations of motor and sensory nerve blockade were similar. This observation is important in that it could be undesirable for motor blockade to last longer than sensory blockade.

The proof-of-concept system described here could undergo numerous modifications to enhance performance in the clinical setting. The intensity and duration of nerve block from any given release event could be extended by the codelivery of drugs that enhance the effectiveness of site 1 sodium-channel blockers, including amino-amide and amino-ester ("conventional") local anesthetics (6, 50, 53), vasoconstrictors (50, 53), and dexmedetomidine (54). The basal release of TTX from the liposomes could be slowed by designing vesicles that can revert to their original state and maintain their physical integrity after irradiation, allowing further triggered events. Triggerability also might be achieved by using a lower, potentially safer, energy dose by coupling the NIR-triggered mechanism with other triggering mechanisms, e.g., photothermal effects (8, 14), reversible chemical reactions (14, 15), or mechanical disturbance (55, 56).

No significant myotoxicity was seen in vivo from the administration and irradiation of liposomes and the resulting release of singlet oxygen. Perhaps it is not surprising that singlet oxygen would not cause toxicity, because it has a lifetime of ~3 μs and a travel distance of ~268 nm in aqueous solution (57). The nanometer-range travel distance is very small compared with the length scale of tissues. There was no neurotoxicity except that one rat in the irradiated Lipo-PS-TTX group had perineural edema, which might have resulted from injury during injection (58, 59).

In conclusion, we have provided proof-of-concept of an externally triggerable nerve block system for adjustable on-demand pain relief. The intensity, duration, and timing of local anesthesia could all be modulated by changing the parameters of irradiation. Tissue reaction (myotoxicity, neurotoxicity, inflammation) was benign.

Methods

Liposome Preparation. Liposomes were prepared by the thin lipid film hydration method as reported (6, 7). The lipid formulation [DSPC (Avanti Polar Lipids), DLPC (Avanti Polar Lipids), DSPG (Genzyme), and cholesterol (Sigma) at molar ratio 3:3:2:3, along with 0.45 mol % (based on total lipid) PS] was dissolved in a solution of chloroform:methanol 9:1. The solvent then was vaporized, and the lipid was redissolved in t-butanol, followed by lyophilization. The lipid cake was hydrated with PBS, TTX solution (0.3 mg/mL PBS; Abcam), or sulforhodamine B solution (50 mg/mL PBS; Aldrich). The suspension was homogenized at 10,000 × *g* for 5 min using a 3/8-in MiniMicro workhead (Silverson) on an L5M-A Laboratory Mixer (Silverson). After 10 freeze–thaw cycles, the solution was dialyzed against PBS for 48 h in a dialysis tube (Spectrum Laboratories) with a molecular mass cutoff of 50 kDa. The formulation of nonphototriggerable liposomes (DSPC-PS-SRho) was DSPC:DSPG:cholesterol at a molar ratio of 6:2:3.

Animal Studies. Animal studies were conducted following protocols approved by the Boston Children's Hospital Animal Care and Use Committee in accordance with the guidelines of the International Association for the Study of Pain (60). Adult male Sprague–Dawley rats (Charles River Laboratories) weighing 325–400 g were housed in groups under a 12-h/12-h light/dark cycle with lights on at 6:00 AM.

After being anesthetized with isoflurane-oxygen, the animals were injected with 200 μL of liposomes using a 23-G needle. The needle was introduced postero-medial to the greater trochanter, pointing in the antero-medial direction, and upon contact with bone the liposomes were injected onto the sciatic nerve (7). The animals were irradiated with a 730-nm laser for the indicated irradiance and duration.

Sensory nerve block was examined at predetermined time points by a modified hotplate test (hind-paw thermal latency) as reported previously (49, 50). The plantar surface of the rat's hind paw was placed on a preheated hot plate at 56 °C. The time until the animal withdrew its foot (the thermal latency) was recorded. Animals that did not retract the foot after 12 s were removed from the hotplate to prevent thermal injury. A thermal latency above 7 s was considered a successful nerve block for the purpose of calculating the duration of nerve block. Measurements were repeated three times at each time interval.

Motor nerve block was assessed by a weight-bearing test to determine the motor strength of the rat's hindpaw, as described previously (49, 50). In brief, the rat was positioned with one hindpaw on a digital balance and was allowed to bear its own weight. The maximum weight that the rat could bear without the ankle touching the balance was recorded, and motor block was considered achieved when the motor strength was less than half-maximal, as described previously (49, 50).

Durations of sensory block were calculated by the time required for thermal latency to return to 7 s, with 2 s as the baseline and 12 s as complete sensory block. The duration of motor block was defined as the time it took for the weight bearing to return halfway to normal from the maximal block (50).

Histology. Animals were killed by carbon dioxide 4 d after the last irradiation event. The sciatic nerve and surrounding tissue were harvested and underwent standard procedures to produce H&E-stained slides. The samples were scored for inflammation (0–4) and myotoxicity (0–6), as reported (35). All scoring and other histological assessments were performed by an observer (A.Y.R.) blinded as to the nature of the individual samples. The inflammation score was a subjective quantification of severity in which 0 was normal and 4 was severe inflammation. The myotoxicity score was determined by the nuclear internalization and regeneration of myocytes, two representative characteristics of local anesthetics' myotoxicity. Nuclear internalization was characterized by myocytes having nuclei located away from their usual location at the periphery of the cell. Regeneration was characterized by the presence of shrunken myocytes with basophilic cytoplasm. The scoring scale was as follows: 0 = normal; 1 = perifascicular internalization; 2 = deep internalization (more than five cell layers); 3 = perifascicular regeneration; 4 = deep tissue regeneration (more than five cell layers); 5 = hemifascicular regeneration; 6 = holofascicular regeneration.

To evaluate the neurotoxicity of the liposomal formulations and light-triggered events, the sciatic nerve samples were fixed in Karnovsky's KII Solution (2.5% glutaraldehyde, 2.0% paraformaldehyde, 0.025% calcium chloride in 0.1 M cacodylate buffer, pH 7.4). Samples were treated with osmium tetroxide for postfixation and subsequently were stained with uranyl acetate, were dehydrated in graded ethanol solutions, and were infiltrated with propylene oxide/TAAB 812 Resin (TAAB Laboratories, Calleva Park, United Kingdom) mixtures. Tissue sections of 0.5 μm were stained with toluidine blue, followed by high-resolution light microscopy (6, 52).

Statistical Analysis. Statistical comparisons of cell viability were performed using the Student *t*-test. To avoid type 1 error in multiple comparisons during the analysis, the Bonferroni correction was used, which corrects the *P* value required for statistical significance (α), determined by dividing 0.05 by the number of comparisons. Four planned comparisons were performed between groups, $\alpha = 0.05/4 = 0.0125$. Statistical significance was determined when the *P* value was <0.0125. The Kruskal–Wallis one-way ANOVA was selected for statistical comparison of the inflammation and myotoxicity scores because of the ordinal character of the scores. Bonferroni correction was performed for 10 planned comparisons to avoid type 1 errors; $\alpha = 0.05/10 = 0.005$. Statistical significance was determined when the *P* value was <0.005.

ACKNOWLEDGMENTS. This work was supported by NIH Grant GM073626 (to D.S.K.).

1. Turk DC (2002) Clinical effectiveness and cost-effectiveness of treatments for patients with chronic pain. *Clin J Pain* 18(6):355–365.
2. Dolin SJ, Cashman JN, Bland JM (2002) Effectiveness of acute postoperative pain management: I. Evidence from published data. *Br J Anaesth* 89(3):409–423.
3. Apfelbaum JL, Chen C, Mehta SS, Gan TJ (2003) Postoperative pain experience: Results from a national survey suggest postoperative pain continues to be undermanaged. *Anesth Analg* 97(2):534–540.
4. Lynch ME, Watson CPN (2006) The pharmacotherapy of chronic pain: A review. *Pain Res Manag* 11(1):11–38.
5. McAlvin JB, Kohane DS (2014) Prolonged duration local anesthesia. *Focal Controlled Drug Delivery, Advances in Delivery Science and Technology*, eds Domb AJ, Khan W (Springer, New York), pp 653–677.
6. Epstein-Barash H, et al. (2009) Prolonged duration local anesthesia with minimal toxicity. *Proc Natl Acad Sci USA* 106(17):7125–7130.
7. Shankarappa SA, et al. (2012) Prolonged nerve blockade delays the onset of neuropathic pain. *Proc Natl Acad Sci USA* 109(43):17555–17560.
8. Timko BP, Dvir T, Kohane DS (2010) Remotely triggerable drug delivery systems. *Adv Mater* 22(44):4925–4943.
9. Timko BP, et al. (2014) Near-infrared-actuated devices for remotely controlled drug delivery. *Proc Natl Acad Sci USA* 111(4):1349–1354.
10. Tong R, Chiang HH, Kohane DS (2013) Photoswitchable nanoparticles for in vivo cancer chemotherapy. *Proc Natl Acad Sci USA* 110(47):19048–19053.
11. Epstein-Barash H, et al. (2010) A microcomposite hydrogel for repeated on-demand ultrasound-triggered drug delivery. *Biomaterials* 31(19):5208–5217.
12. Hoare T, et al. (2011) Magnetically triggered nanocomposite membranes: A versatile platform for triggered drug release. *Nano Lett* 11(3):1395–1400.
13. Huang Z (2005) A review of progress in clinical photodynamic therapy. *Technol Cancer Res Treat* 4(3):283–293.
14. Tong R, Kohane DS (2012) Shedding light on nanomedicine. *Wiley Interdiscip Rev Nanomed Nanobiotechnol* 4(6):638–662.
15. Shum P, Kim JM, Thompson DH (2001) Phototriggering of liposomal drug delivery systems. *Adv Drug Deliv Rev* 53(3):273–284.
16. Rwei AY, Wang W, Kohane DS (2015) Photoresponsive nanoparticles for drug delivery. *Nano Today*, 10.1016/j.nantod.2015.06.004.
17. Welch AJ, van Gemert MJC (2011) *Optical-Thermal Response of Laser Irradiated Tissue* (Springer, New York), 2nd Ed, pp 267–319.
18. Soldatova AV, et al. (2011) Near-infrared-emitting phthalocyanines. A combined experimental and density functional theory study of the structural, optical, and photophysical properties of Pd(II) and Pt(II) α-butoxyphthalocyanines. *Inorg Chem* 50(3):1135–1149.
19. Rihter BD, Kenney ME, Ford WE, Rodgers MAJ (1990) Synthesis and photoproperties of diamagnetic octabutoxyphthalocyanines with deep red optical absorbance. *J Am Chem Soc* 112(22):8064–8070.
20. Vasdekis AE, Scott EA, O'Neil CP, Psaltis D, Hubbell JA (2012) Precision intracellular delivery based on optofluidic polymersome rupture. *ACS Nano* 6(9):7850–7857.
21. Halliwell B, Chirico S (1993) Lipid peroxidation: Its mechanism, measurement, and significance. *Am J Clin Nutr* 57(5, Suppl):715S–724S, discussion 724S–725S.
22. Harding LB, Goddard WA (1980) The mechanism of the ene reaction of singlet oxygen with olefins. *J Am Chem Soc* 102(2):439–449.
23. Wang Y, Xu H, Zhang X (2009) Tuning the amphiphilicity of building blocks: Controlled self-assembly and disassembly for functional supramolecular materials. *Adv Mater* 21(28):2849–2864.
24. Evans DF (1988) Self-organization of amphiphiles. *Langmuir* 4(1):3–12.
25. Randles EG, Bergethon PR (2013) A photodependent switch of liposome stability and permeability. *Langmuir* 29(5):1490–1497.
26. Pashkovskaya A, et al. (2010) Light-triggered liposomal release: Membrane permeabilization by photodynamic action. *Langmuir* 26(8):5726–5733.
27. Steiner R (2011) Laser-tissue interactions. *Laser and IPL Technology in Dermatology and Aesthetic Medicine*, eds Raulin C, Karsai S (Springer, Berlin), pp 23–36.
28. Cheong W-F, Prahl SA, Welch AJ (1990) A review of the optical properties of biological tissues. *IEEE J Quantum Electron* 26(12):2166–2185.
29. Simpson CR, Kohl M, Essenpreis M, Cope M (1998) Near-infrared optical properties of ex vivo human skin and subcutaneous tissues measured using the Monte Carlo inversion technique. *Phys Med Biol* 43(9):2465–2478.
30. Weissleder R (2001) A clearer vision for in vivo imaging. *Nat Biotechnol* 19(4):316–317.
31. Yamamoto Y, Niki E, Kamiya Y, Shimasaki H (1984) Oxidation of lipids. 7. Oxidation of phosphatidylcholines in homogeneous solution and in water dispersion. *Biochim Biophys Acta* 795(2):332–340.
32. Fukuzawa K, Inokami Y, Tokumura A, Terao J, Suzuki A (1998) Singlet oxygen scavenging by α-tocopherol and β-carotene: Kinetic studies in phospholipid membranes and ethanol solution. *Biofactors* 7(1-2):31–40.
33. Frankel EN (1984) Chemistry of free radical and singlet oxidation of lipids. *Prog Lipid Res* 23(4):197–221.
34. Tanielian C, Mechin R (1994) Reaction and quenching of singlet molecular oxygen with esters of polyunsaturated fatty acids. *Photochem Photobiol* 59(3):263–268.
35. Padera RF, Tse JY, Bellas E, Kohane DS (2006) Tetrodotoxin for prolonged local anesthesia with minimal myotoxicity. *Muscle Nerve* 34(6):747–753.
36. Sakura S, Bollen AW, Ciriales R, Drasner K (1995) Local anesthetic neurotoxicity does not result from blockade of voltage-gated sodium channels. *Anesth Analg* 81(2):338–346.
37. Mallick S, Choi JS (2014) Liposomes: Versatile and biocompatible nanovesicles for efficient biomolecules delivery. *J Nanosci Nanotechnol* 14(1):755–765.
38. Chang H-I, Yeh M-K (2012) Clinical development of liposome-based drugs: Formulation, characterization, and therapeutic efficacy. *Int J Nanomedicine* 7:49–60.
39. Fozzard HA, Lipkind GM (2010) The tetrodotoxin binding site is within the outer vestibule of the sodium channel. *Mar Drugs* 8(2):219–234.
40. Lodish HBA, et al. (2000) 3 Biomembranes: Structural organization and basic functions. *Molecular Cell Biology* (W. H. Freeman, New York), 4th Ed.
41. Kang SN, et al. (2013) Enhancement of liposomal stability and cellular drug uptake by incorporating tributyrin into celecoxib-loaded liposomes. *Asian Journal of Pharmaceutical Sciences* 8(2):128–133.
42. Ohkawa H, Ohishi N, Yagi K (1978) Reaction of linoleic acid hydroperoxide with thiobarbituric acid. *J Lipid Res* 19(8):1053–1057.
43. Kiwi J, Nadtochenko V (2004) New evidence for TiO2 photocatalysis during bilayer lipid peroxidation. *J Phys Chem B* 108(45):17675–17684.
44. Gross E, Ehrenberg B, Johnson FM (1993) Singlet oxygen generation by porphyrins and the kinetics of 9,10-dimethylanthracene photosensitization in liposomes. *Photochem Photobiol* 57(5):808–813.
45. Lavi A, Weitman H, Holmes RT, Smith KM, Ehrenberg B (2002) The depth of porphyrin in a membrane and the membrane's physical properties affect the photosensitizing efficiency. *Biophys J* 82(4):2101–2110.
46. Gomes A, Fernandes E, Lima JLFC (2005) Fluorescence probes used for detection of reactive oxygen species. *J Biochem Biophys Methods* 65(2-3):45–80.
47. Chmielarz B, Bajdor K, Labudzinska A, Klukowska-Majewska Z (1995) Studies on the double bond positional isomerization process in linseed oil by UV, IR and Raman spectroscopy. *J Mol Struct* 348:313–316.
48. Klamt A (1996) Calculation of UV/Vis spectra in solution. *J Phys Chem* 100(9): 3349–3353.
49. Thalhammer JG, Vladimirova M, Bershadsky B, Strichartz GR (1995) Neurologic evaluation of the rat during sciatic nerve block with lidocaine. *Anesthesiology* 82(4):1013–1025.
50. Kohane DS, et al. (1998) A re-examination of tetrodotoxin for prolonged duration local anesthesia. *Anesthesiology* 89(1):119–131.
51. Feirabend HKP, Choufoer H, Ploeger S (1998) Preservation and staining of myelinated nerve fibers. *Methods* 15(2):123–131.
52. McAlvin JB, et al. (2014) Multivesicular liposomal bupivacaine at the sciatic nerve. *Biomaterials* 35(15):4557–4564.
53. Adams HJ, Blair MRJ, Jr, Takman BH (1976) The local anesthetic activity of tetrodotoxin alone and in combination with vasoconstrictors and local anesthetics. *Anesth Analg* 55(4):568–573.
54. McAlvin JB, et al. (2015) Corneal anesthesia with site 1 sodium channel blockers and dexmedetomidine. *Invest Ophthalmol Vis Sci* 56(6):3820–3826.
55. Schroeder A, Kost J, Barenholz Y (2009) Ultrasound, liposomes, and drug delivery: Principles for using ultrasound to control the release of drugs from liposomes. *Chem Phys Lipids* 162(1-2):1–16.
56. Huebsch N, et al. (2014) Ultrasound-triggered disruption and self-healing of reversibly cross-linked hydrogels for drug delivery and enhanced chemotherapy. *Proc Natl Acad Sci USA* 111(27):9762–9767.
57. Skovsen E, Snyder JW, Lambert JDC, Ogilby PR (2005) Lifetime and diffusion of singlet oxygen in a cell. *J Phys Chem B* 109(18):8570–8573.
58. Gentili F, Hudson AR, Hunter D, Kline DG (1980) Nerve injection injury with local anesthetic agents: A light and electron microscopic, fluorescent microscopic, and horseradish peroxidase study. *Neurosurgery* 6(3):263–272.
59. Hogan QH (2008) Pathophysiology of peripheral nerve injury during regional anesthesia. *Reg Anesth Pain Med* 33(5):435–441.
60. Zimmermann M (1983) Ethical guidelines for investigations of experimental pain in conscious animals. *Pain* 16(2):109–110.